

### **Audio Engineering Society**

## Convention Paper 10465

Presented at the 150th Convention 2021 May 25–28, Online

This convention paper was selected based on a submitted abstract and 750-word precis that have been peer reviewed by at least two qualified anonymous reviewers. The complete manuscript was not peer reviewed. This convention paper has been reproduced from the author's advance manuscript without editing, corrections, or consideration by the Review Board. The AES takes no responsibility for the contents. This paper is available in the AES E-Library (http://www.aes.org/e-lib), all rights reserved. Reproduction of this paper, or any portion thereof, is not permitted without direct permission from the Journal of the Audio Engineering Society.

# Auralizing concert venues over extended listening areas using wave field synthesis

Jonas Braasch<sup>1</sup>, Samuel Chabot<sup>1</sup>, Evan Chertok<sup>1</sup>, Jonathan Mathews<sup>1</sup>, and E.K. Ellington Scott<sup>1</sup>

<sup>1</sup>School of Architecture, Rensselaer Polytechnic Institute, Troy, NY, 12180, USA

Correspondence should be addressed to Jonas Braasch (braasj@rpi.edu)

#### **ABSTRACT**

This paper proposes an efficient method to create auralizations of acoustical landmarks using a 2D ray-tracing algorithm and publicly available floor plans for a 128-channel wave field synthesis (WFS) system with 2.5D approximation. Late reverberation parameters are calculated using additional volumetric data. The approach allows the rapid sonic recreation of historical concert venues with adequate sound sources. The listeners can walk through these recreations over an extended user area  $(12 \times 10 \text{ sqm})$ , and the software suite can be used to calculate room acoustical parameters for various positions directly using a binaural rendering method or via the WFS simulation.

#### 1 Introduction

Room Acousticians typically rely on impulse responses when characterizing or auralizing acoustical interior spaces, such as concert halls, churches, mosques, and other venues. The concept of impulse responses in the time domain, or the corresponding transfer functions in the frequency domain, has a long tradition in electronic circuits. It is an adequate method to describe linear, time-invariant systems with defined in- and outputs, for example, those found in audio amplifiers. While acoustical enclosures can be treated as linear, time-invariant (LTI) systems, they do not have defined in- and outputs. In practice, the latter is addressed by creating in- and outputs at selected source and receiver positions. This can be done in the form of a loudspeaker/microphone pair that is placed in a venue to measure the roomimpulse response between these two positions. Such an

approach has become very popular in audio engineering practice using so-called convolution reverbs that use the convolution method to process sufficiently dry audio files as if they had been recorded in the room at the microphone position the impulse response was captured [1]. Alternatively, source and receiver positions can be defined in a computer-generated space, as will be done in this paper.

One problem of this practice is that while we capture how the room sounds for the chosen source/receiver positions, we do not learn much about how the room sounds as a whole. For example, this method does not allow us to "walk" through a room to explore acoustical changes in different positions. Nearly all auralization techniques, be they headphone-based or loudspeaker-based, are built on the idea of distinct source/receiver positions confining the listening area to a small sweet spot – the area where spatial sound is accurately re-

produced. Wave-field synthesis (WFS) is a notable exception to the sweet-spot restricting spatial-audio methods. Here, Huygen's (1690) concept of elementary waves [2] and Fresnel's principle of interference (1819) [3] are used to simulate the rectilinear propagation of sound waves using a large array of loudspeakers to simulate secondary sources of a virtual sound source behind the array. The method allows to accurately reproduce sound across larger listening areas below a spatial aliasing frequency. A research team at Delft University was the first to design and implement a WFS system in practice [4, 5]. Already in the 1930s, Steinberg and Snow followed a similar idea, using a linear "curtain" of equidistant microphones to capture a wavefront and reproducing the latter at a remote site with loudspeakers spaced at the same distances [6].

While much research has been devoted to reproduce sound waves emitted from direct sound sources accurately [7, 8], comparatively little focus has been set on the faithful reproduction of sound reflected from boundaries [9]. Instead, wall reflections are often simulated using traditional stereophonic methods or spherical harmonics, but methods that built on a single point-like receiver position. While in practice, the sweet spot area can be quite large using these methods, they still attempt to simulate a room from a single perspective.

The goal of the paper presented here was to create walkable room simulations over an extended listening area. The concept uses a 2D method to render the direct sound signals and early reflections, a feasible approach considering that wave field synthesis (WFS) systems are usually 2D setups, where loudspeakers are placed along the perimeter of an extended listener area. The proposed method is compatible with the 2.5D operator for WFS. The system is primarily used to recreate historic architectural venues from antiquity to today so that listeners can experience these venues' acoustical footprint over the extended floor area (10  $\times$ 12 sqm) of Rensselaer's Collaborative Research Augmented Immersive Virtual Environment (CRAIVE-Lab). The CRAIVE-Lab uses 134 full-range loudspeakers (JBL 308, 128 speakers along the lab's perimeter at ear height, plus six ceiling speakers). Eight short-throw front projectors reproduce congruent immersive 360deg images, e.g., HDR panoramic photos, on a screen that encloses the listening area up to a height of 4.3 m. The screen is microperforated for improved acoustic performance. This makes the CRAIVE-Lab a unique

venue for auralizations, given that typical CAVE systems have hard projection surfaces. The latter create audible room reflections that superimpose with the simulated room reflections of the WFS signals. The floor area of the CRAIVE-Lab is also more extensive than that of a typical CAVE. The lab can host up to 49 participants at a time (restricted by fire code), providing the opportunity to experience an extended section of the simulated acoustical enclosure acoustically. The proposed method allows users to auralize historic buildings from scaled floor plans, which are – in contrast to full three-dimensional CAD models – often publicly available. The research started from an educational angle, and much of the description in this paper still reflects this original goal.

In the next section, the basic concept of our proposed auralization technique is discussed, followed by auralization examples that are described in Section 2. The paper concludes with a brief conclusion and outlook section.

#### 2 Methods & Implementation

Figure 1 shows the system architecture of the ray-tracing program. All input variables and data are shown at the bottom. The basis for auralizing a building or outdoor venue is a floor plan with a scale or known dimensions. Further, a database with wall and floor materials is utilized to determine absorption coefficients. The user determines the locations of sound sources and receivers and provides sufficiently anechoic sound files for auralization. The receiver positions determine the locations of virtual microphones for the WFS loudspeaker locations, the location of a virtual dummy head (rendered through head-related transfer functions), or the position of a virtual spherical microphone array.

#### 2.1 Floor-plan annotation

The first step in the auralization process is the annotation of floor plans. Standard floor plans such as those found on the world wide web can be processed as long as the user has information about its dimensions in the form of a scale or known overall dimension of the building (e.g., length and width). If needed, dimensions can also be estimated from satellite data or street maps. For the auralization preparation, the user marks up a floor plan using a bitmap editor (e.g., GIMP or Photoshop), annotating corners with red dots and columns

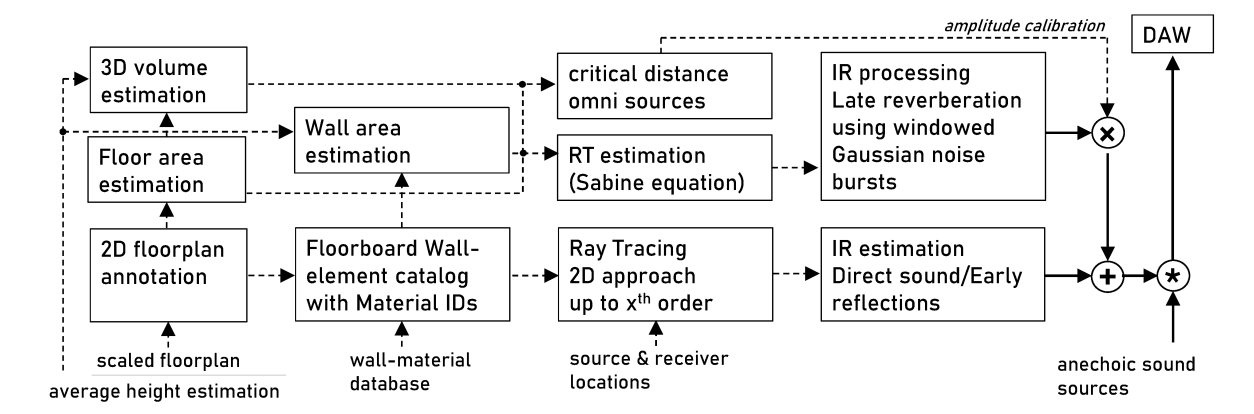


**Fig. 1:** System architecture for the auralization algorithm.

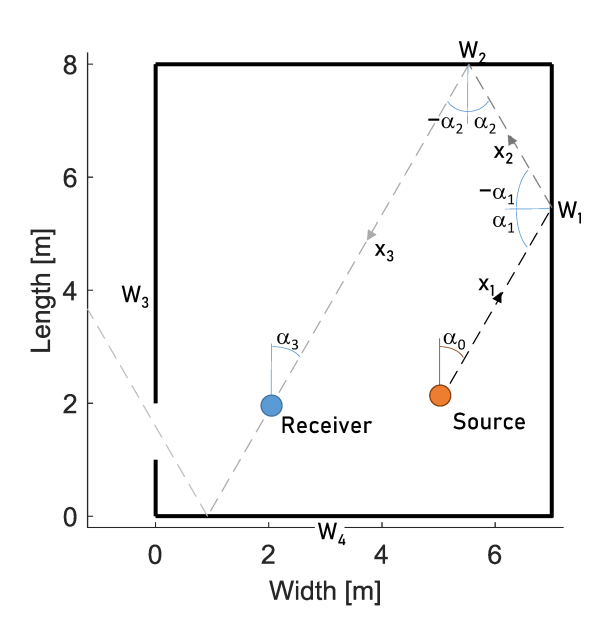


Fig. 2: Example of ray-tracing pathway.

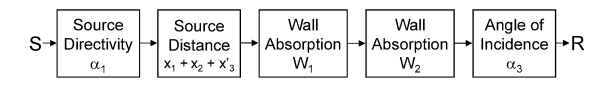


Fig. 3: Ray-tracing signal flow.

with green dots. Further, the floor plan scale has to be annotated, and the original dimensions need to be handed over to the program as well, for example, 0 m and 5 m for two scale points. The auralization program automatically enumerates the corner positions and creates pairs of corners spanning wall elements. The user corrects and edits these pairs to finalize the digitized floor plan.

The user can either assign a single wall-material ID to all walls or specify individual wall-material IDs for each wall – see Fig. 1, bottom, 2<sup>nd</sup>-from-left box. Currently, wall material data is taken from a DIN database, and the database contains a short description of the material, frequency-specific absorption coefficients and Finite-Impulse-Response (FIR) filter coefficients. The latter is needed to compute adequate room impulse responses.

#### 2.2 Ray-tracing algorithm

For each sound-source position, the program sends out rays at equidistant azimuth angles covering the full horizontal plane (360° circle) – see Fig. 1,  $3^{rd}$ -left bottom box. Intersection points are computed for each ray and boundary object using the solution of the line–line intersection problem in Euclidean geometry. For each ray, the closest boundary intersection is determined. At the intersections, the reflection angle is calculated using Ibn Sahl/Snell's law [10, 11], which predicts that the reflected angle measured from the normal of a plane surface equals the incoming angle:  $\cos(\alpha_r) = \cos(\alpha_i)$ , and the next order ray is sent out into the new direction

until the maximum order (e.g., the number of reflections) specified by the user is reached or the ray exits the floor plan – see Fig. 2. The outgoing rays are stored as a sequence of ray elements containing the intersection points and the boundary material identifiers. Since the initial angles are stored with the rays, a source-specific directivity pattern can be simulated after all rays have been traced.

#### 2.2.1 Creating a room impulse response

Next, the rays are collected by receivers in the module IR estimation – see Fig. 1, rightmost bottom box. Receivers can be located anywhere in the rendered room. For WFS, a virtual array is placed into the floor plan section that should be auralized. The receivers (virtual microphones) are positioned at the WFS loudspeaker positions. So for a 128-channel loudspeaker system, 128 receivers are placed at the loudspeaker positions. For each receiver, a separate impulse response is created. To catch the rays, a virtual circle with an adjustable diameter is positioned at each receiver location. Then, the algorithm calculates which ray elements intersect the circle, and for all positive cases, the total ray distance between sound source and receiver is calculated. All listed values are stored together with the final angle of incidence, the angle the ray was initially sent out, the reflection order, and the sequence of wall identifiers. Based on these data, the impulse response is computed. The direct sound and reflections are computed as delta peaks at the delays that correspond to the rays' path length from the source to the receiver. In addition, each impulse is transformed the following way – see also Fig. 3:

- 1. The intensity of the ray is reduced based on the inverse-square law. Consequently, the sound pressure magnitude decreases with 1/r.
- 2. The high frequencies are filtered out based on dissipation effects in air.
- 3. The absorption effects of the walls and other boundaries are simulated using a cascaded Finite Impulse Response (FIR) filter. The material-specific filters are chosen from a DIN database [12]. The number of cascaded filters matches the order of the reflection.

4. In the final step, incoming direct sound and reflections are selected by their close proximity passing a receiver position within the virtual circle that was placed around it. The virtual receivers are directionally sensitive using the positive lobe of a figure-of-eight pattern. The latter points outward the array to avoid echo artifacts resulting from rays passing through the array at the opposite end of the array. An overlap-add method ensures that the delayed reflections can partially overlap, which can happen because of the cascading FIR filters' prolonged effect that simulates the wall reflections.

#### 2.2.2 Simulation of late reverberation

Late diffuse reverberation is computed in addition to the early reflections generated by the ray-tracing model. This process is described in Fig. 1 (second and third rows from bottom). In order to calculate the frequency-specific reverberation times via the Sabine equation, we first need to calculate the volume as well as the individual areas of walls, floor, and ceiling. For this purpose, the average height of the enclosure has to be calculated or estimated – see Fig. 1, bottom/left. The floor area  $A_F$  (center-left box in Fig. 1) is calculated from the annotated floor plan and multiplied with the average height h to estimate the volume:  $V = A_F \cdot h$ . (top-left box in Fig. 1). The wall areas are estimated as the product of the average height and wall-element length – see Fig. 1, top,  $2^{\rm nd}$ -left box.

Using these dimensions, as well as the absorption coefficients the frequency-specific reverberation times are computed via the Sabine equation:

$$T_{60} = 0.161 \cdot V / (A + 4m \cdot V)$$
s. (1)

The total absorption, A, is defined as the sum of all surface elements  $S_n$  multiplied with their specific absorption coefficient  $\alpha_n$ :

$$A = \left(\sum_{k=1}^{K} \alpha_k \cdot S_k\right). \tag{2}$$

Since the late reverberation tail is formed by a stochastic process with an underlying Gaussian distribution, the fine structure of the simulated reverb tail is constructed from a Gaussian noise sample. The duration

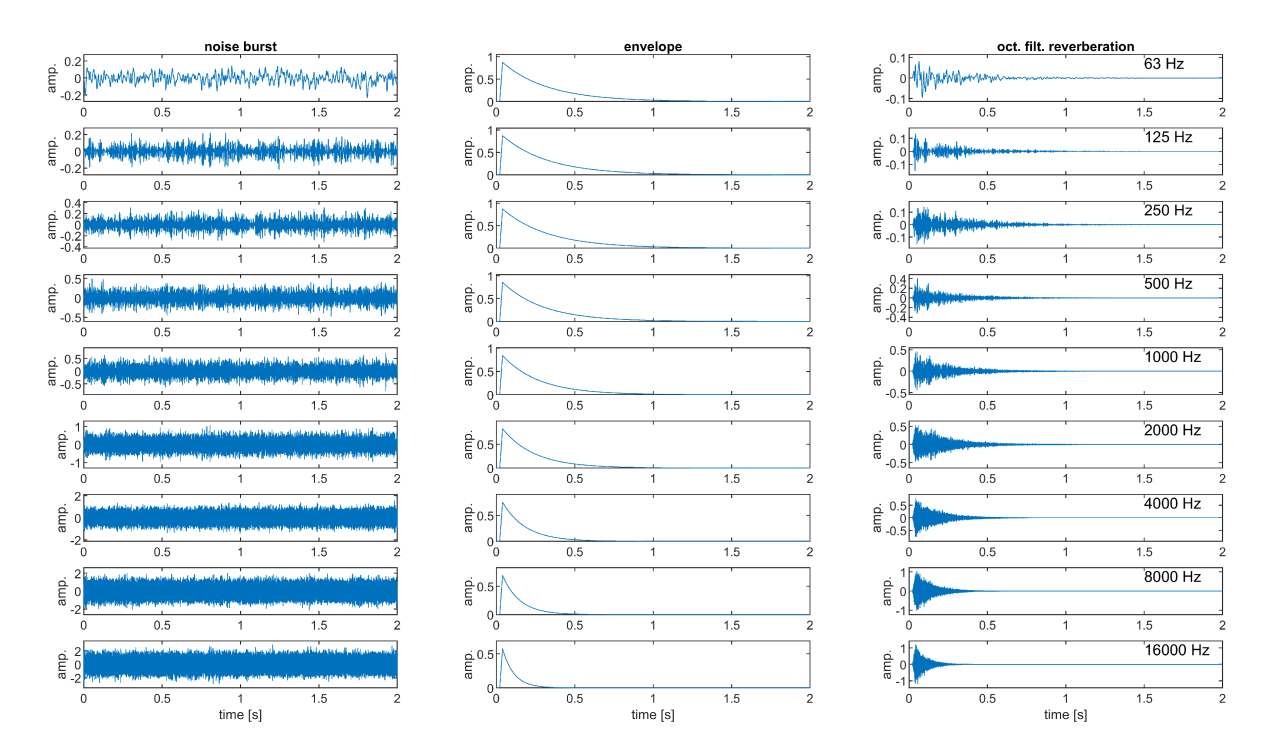


**Fig. 4:** Process to create artificial reverberation impulse responses from octave-wide Gaussian noise bursts (left column) that are windowed using exponentially-decaying envelopes (center column) to create octave-filtered noise-like impulse responses (right column). The latter are summed up for the final impulse response. Each row depicts a different octave-band as indicated.

of the Gaussian noise sample is adjusted to twice the value of the maximum reverberation time. Next, the noise sample is processed through an octave-band filter bank with nine bands – see Fig. 4, left column. An exponentially-decaying window,  $y_k$ , adjusted to the frequency-specific reverberation time, is calculated for each octave band k:

$$y_k = e^{\frac{-t \cdot 20 \cdot \log(10)}{T_{60,k} \cdot 60}},$$
 (3)

with the reverberation time,  $T_{60,k}$ , in the  $k^{th}$  frequency band, and the time, t, in seconds. Afterwards, the total exponentially-decaying noise signal,  $x_t$ , is reassembled by summing the octave-filtered noise samples multiplied with the exponentially decaying window sample by sample:

$$x_t = \sum_{k=1}^K x_k \cdot y_k. \tag{4}$$

The process is repeated for each loudspeaker channel using independent Gaussian noise samples for each channel while keeping all other parameters constant. It has been shown that the described method benefits from having a large number of independent reverberation channels [13].

The absorptive surface area is calculated from the raytracing model's wall elements; each multiplied with the average height. The frequency-specific absorption coefficients are determined through the values stored in the DIN database via the wall material identifiers. A linear onset ramp is calculated to gradually blend in the late reverberation tail with the direct sound and early reflections. The onset ramps' start and end points can be adjusted by the user.

Two methods are available to calculate the direct-toreverberant energy ratio. The first method estimates the critical distance, the distance from the sound source at which the sound pressure levels of the direct sound matches the sound pressure level of the reverberant field. For an omnidirectional sound source, the critical distance can be calculated using this equation [14, p. 317]:

$$r_c = 0.057 \cdot \sqrt{\frac{\gamma V}{T_{60}}},\tag{5}$$

with the volume, V, the reverberation time,  $T_{60}$ , and the directivity factor,  $\gamma$ . For an omnidirectional sound source that we will assume in the subsequent calculation, the directivity factor is one.

In the next step, the impulse response is calculated at a receiver position at the critical distance. The overall energy of the impulse response,  $E_T$ , is the sum of the direct sound energy,  $E_D$ , the early reflection energy,  $E_E$ , as well as the late reverberant energy,  $E_L$ :

$$E_T = E_D + E_E + E_L. (6)$$

At the critical distance, the following condition has to be met for an omnidirectional source and receiver pair:

$$E_D = E_E + E_L. (7)$$

Consequently, the energy of the late reverberation has to be adjusted to:

$$E_L = E_D - E_E, (8)$$

$$E_{L} = E_{D} - E_{E},$$

$$\sum_{t=0}^{2T_{60}} p_{L}^{2} = \sum_{t=0}^{2T_{60}} p_{D}^{2} - \sum_{t=0}^{2T_{60}} p_{E}^{2},$$
(8)

with the sound pressure, p, which is, of course, proportional to the digital signal amplitude.

In the second method, the exponentially-decaying amplitude of the reverberation tail is fitted to the exponentially-decaying amplitudes of the reflection pattern. For this purpose, both signals are logarithmized so the decaying impulse response can be fitted by a linear regression curve. The amplitudes of the decaying slope are then matched, and a cross-fade method is used to blend out the early reflections while gradually blending in the late reverberation.

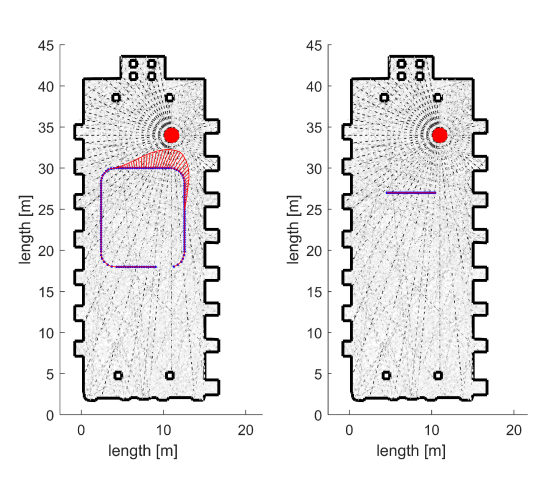


Fig. 5: Raytracing results for the Haydnsaal in Eisenstadt. The left graph shows the simulation using a WFS array for the CRAIVE-Lab, the right graph depicts the same condition but for a virtual line array.

#### **Auralization Examples**

This section deals with concrete auralization examples that were established using the raytracing method described in the previous sections.

#### Haydnsaal, Eisenstadt

The first example is a recreation of the Great Hall of Schloss Esterházy (now Haydnsaal), where Joseph Haydn inaugurated several of his symphonies. The hall is located in Eisenstadt (now Austria) at the seat of the Esterházy family that Haydn worked for. The hall was built during the baroque building phase of the castle (1663-1672). The floor plan was scanned and manually annotated from Jürgen Meyer's paper on Haydn's concert venues [15]. The virtual receivers for the WFS loudspeaker locations are depicted in blue in the left graph of Fig. 5. A virtual sound source was positioned at the top right corner, indicated by the red filled circle.

The right graph shows the same condition but for a virtual microphone array that was used for analysis purposes. The virtual line array consists of 40 microphones with 15-cm spacing between adjacent microphones. In the following, we will compare two conditions. In the first conditions, we analyze the simulated output of the virtual microphone array directly by performing the

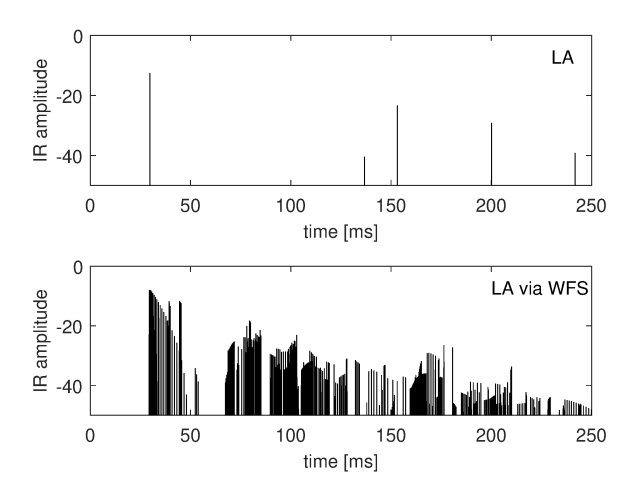


**Fig. 6:** Simulated impulse responses for the Haydnsaal in Eisenstadt, Austria. The top graph shows the results for the direct line-array analysis, the bottom graph the result for the intermediate WFS rendering method. Both graphs show the results for the direct and early reflections in the absence of the late reverberation. See main text for details.

auralization process directly for the line array receivers. In the second condition, the auralization will be first performed for the WFS array, using these locations as receivers. In a subsequent step, the outputs of the WFS array are processed as if they were captured by the line array receivers. For this purpose, the output of each of the 128 WFS channels is delayed and attenuated according to the distances between a virtual line array receiver and each of the 128 WFS sources. Consequently, each virtual line-array microphone will receive input from all of the 128 WFS channels.

Figure 6 shows impulse-response examples for both conditions. The top graph shows the impulse response for a center line-array receiver (ID #20) for the direct analysis method – see also the right graph in Fig. 5. The first peak shows the direct signal and the subsequent peaks depict early reflections. As expected from the ray-tracing algorithm, the initial reflection pattern is sparse.

The bottom graph of Fig. 6 depicts the condition in which the signal is transformed via the WFS array – see the geometrical configuration in the left graph in Fig. 5. The line array position for the second step is identical to the one shown in the right graph of 5. For

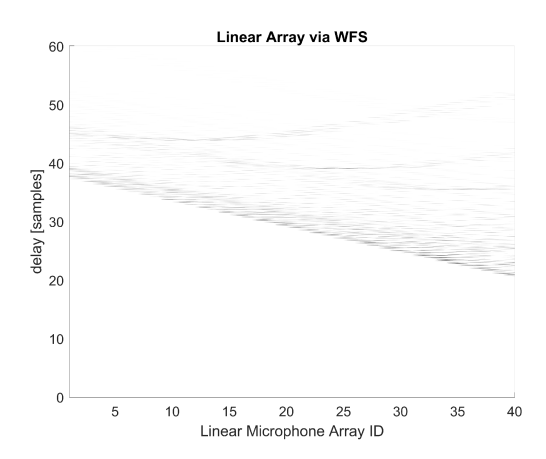


Fig. 7: Impulse responses of all 40 line-array receivers for the Haydnsaal simulation, from left to right with increasing microphone ID (The microphone IDs are counted from left to right). The y-axis shows the time course of the impulse responses. Dark areas show intervals of high acoustic intensity, white areas the lack thereof. The data is shown for the condition with intermediate WFS simulation. See main text for details.

this condition, the reflection pattern is much denser, which is easily explained by the multiple pathways between each WFS source and line array receiver.

Figure 7 depicts the discussed effect further. It shows how the first wavefronts of direct signal and early reflections are followed by "shadow" sound sources from other secondary sound sources (WFS sources). We plan to investigate the perceptual effects of these artifacts in the future. It can be assumed that the precedence effect will play a role here, and the effect might not be as audible as the graphs suggest. Given that a ray-tracing model produces idealized, delta-peak-like reflections, the effect might also have a positive perceptual impact because natural reflections are not as distinct in time as a ray-tracing model predicts.

## 3.2 Acoustical Recreation of the Dan Harpole Cistern

The second auralization example focuses on an acoustical enclosure used for avantgarde music. The Dan Harpole Cistern was built in 1907 as an underwater tank for Fort Worden, WA, to provide water to extinguish

fires that result from enemy attacks. Its substantial volume of 2-million-US gallons (7,600 m³) provides an anecdotally reported reverberation time of 45 seconds. The construction of Fort Worden occurred between 1898 and 1917. Together with Fort Flagler and Fort Casey, it served as a system of three forts called the "The Triangle of Fire" to defend the Pacific coast. It has been named after Admiral John L. Worden and was an active military installation until 1953. It is now a recreational park for the State of Washington.

Interestingly, the underwater tank received its acoustical significance after its official purpose after the emptied tank had been discovered by visiting artists. In June 2007, the tank was named Dan Harpole Cistern to honor the name-giver for his efforts to obtain a designation as "Washington's Official Instrument" for the cistern [16]. The Dan Harpole Cistern has been a recording venue for several landmark recordings, starting with an album from 1989 by Pauline Oliveros, Stuart Dempster, and Panaotis called *Deep Listening*. The Dan Harpole Cistern has a diameter of 186 feet and a floor-to-ceiling height of 14 feet. It is made of concrete and contains 89 square columns (about 15 inches wide).

An impulse response of the cistern was recorded for the 1991 Deep Listening album: *The Ready Made Boomerang*. The following reverberation times were computed from analyzing this impulse response (frequency in kHz, reverberation times in seconds):

The reverberation time is longer than 45 seconds at very low frequencies and much shorter at high frequencies. Usually, circular buildings are often troublesome because they have focused echoes, especially for sound sources at the center. This is actually how whispering galleries work. The high number of columns saves the acoustics of the cistern by creating a high level of diffusion. Jürgen Meyer has pointed out the importance of columns in churches, and they have a similar effect in the Dan Harpole Cistern. There were no adequate absorption coefficients in the DIN database (smooth unpainted concrete), but they were listed in Michael Vorländer's book [17].

Based on the geometrical data, the volume was estimated to be 10,770 m<sup>3</sup>. The value is larger than the volume of 7,600 m<sup>3</sup> (2-million US gallons) provided in the literature. However, it is not clear if the cistern was

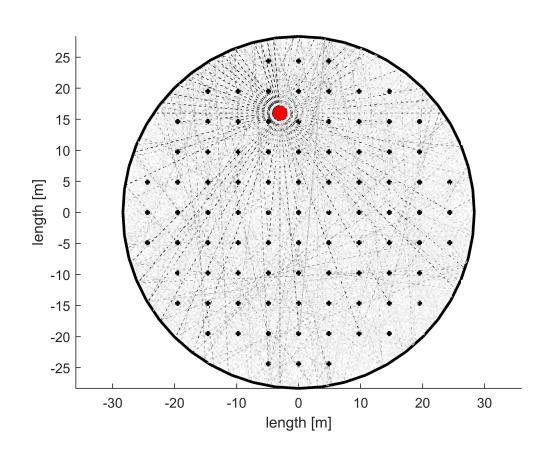


Fig. 8: Raytracing results for the Dan Harpole Cistern.

fully filled with water or if the 2-million US gallons are a rough estimate.

The following values were obtained from the geometrical model using the Sabine equation:

These critical distances were estimated in meters:

Since the estimated reverberation times are too short in the low-frequency range, absorption coefficients were computed for 250 Hz and 1000 Hz. For 1000 Hz, an absorption coefficient of 0.015 produces a reverberation time of 18.3 seconds. For 250, an absorption value of 0.0066 results in a reverberation time of 41.6 seconds. These values correspond to critical distances 0.91 of and 1.38 meters.

Figure 8 shows the result of the ray tracing process for the cistern. The simulated impulse response is plotted in Fig. 9.

#### 4 Conclusion & Outlook

A rapid auralization method was proposed in this paper. Using annotated floor plans and a ray-tracing method, the process allows rapid prototyping of acoustical enclosures. It usually takes less than an hour to annotate the floor plan for a project and about another hour to render the impulse responses and create the auralizations for a brief demo with eight sound

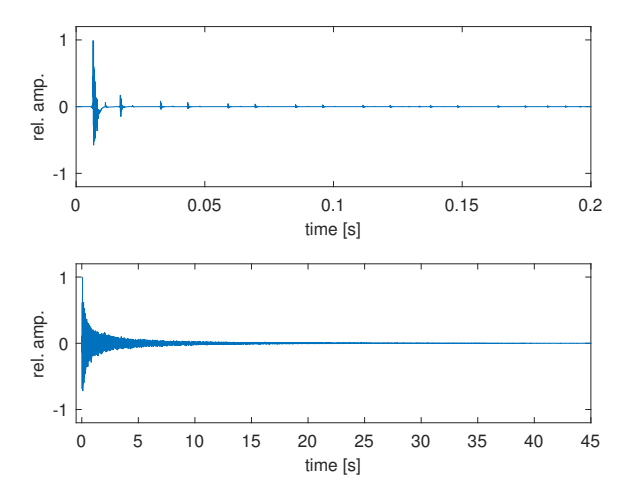


**Fig. 9:** Simulated impulse responses for the Dan Harpole Cistern. The top graph shows the results for the direct sound and early reflection. The bottom graph depicts the results for the late reverberation.

sources and 128 loudspeakers on a typical desktop computer. The growing library of simulated venues also includes the Cologne Cathedral, Savoy Ballroom Jazz Club, Columbia 30<sup>th</sup> Street Studio, St. Mark's cathedral in Venice, St. Patrick's Cathedral in New York City, Pantheon in Rome, Amphitheatre in Trier, to name a few. The software is used regularly in the first author's *Aural Architecture* class, where each student creates his/her own project. The ray-tracing program can also render binaural impulse responses using HRTFs for the analysis of acoustical parameters.

In the future, we plan to complement the method with a binaural model that can be placed virtually into the simulated spaces to analyze and optimize the output of the auralization engine. We also plan to use the binaural model in conjunction with a binaural manikin that will be deployed in the CRAIVE-Lab.

#### Acknowledgement

This material is based upon work supported by the National Science Foundation under Grant Nos. CNS-1229391 and HCC-1909229. The research presented in this paper was carried out within Rensselaer Polytechnic Institute's Cognitive and Immersive Systems Laboratory, a collaboration between RPI and IBM.

#### References

- Braasch, J., "Convolution, Fourier Analysis, Cross-Correlation and their Interrelationship," in R. Bader, editor, *Springer Handbook of Systematic Musicology*, pp. 273–284, Springer, Cham, Switzerland, 2018.
- [2] Huygens, C., Traité de la lumière où sont expliquées les causes de ce qui luy arrive dans la reflexion, dans la refraction, et particulierement dans l'etrange refraction du cristal d'Islande [Treatise on light in which are explained the causes of that which occurs in reflection, in refraction, and particularly in the strange refraction of Iceland spar], chez Pierre Vander Aa marchand libraire, 1690.
- [3] Fresnel, A., "Mémoire sur la diffraction de la lumière [Memorandum on light diffraction]," *Mémoires de l'Académie des Sciences, da p. 339 a p. 475: 1 tav. ft; AQ 21*, p. 339, 1819.
- [4] Berkhout, A. J., de Vries, D., and Vogel, P., "Acoustic control by wave field synthesis," *The Journal of the Acoustical Society of America*, 93(5), pp. 2764–2778, 1993.
- [5] Berkhout, A. J., "A holographic approach to acoustic control," *Journal of the audio engineering society*, 36(12), pp. 977–995, 1988.
- [6] Steinberg, J. C. and Snow, W. B., "Auditory Perspective Physical Factors," *Electrical Engineering*, Jan, pp. 12–17, 1934.
- [7] Spors, S., Rabenstein, R., and Ahrens, J., "The theory of wave field synthesis revisited," in *In 124th Convention of the AES*, Citeseer, 2008.
- [8] Ziemer, T., "Wave field synthesis," in *Springer handbook of systematic musicology*, pp. 329–347, Springer, 2018.
- [9] Hulsebos, E., de Vries, D., and Bourdillat, E., "Improved microphone array configurations for auralization of sound fields by wave-field synthesis," *Journal of the Audio Engineering Society*, 50(10), pp. 779–790, 2002.
- [10] Rashed, R., "A pioneer in anaclastics: Ibn Sahl on burning mirrors and lenses," *Isis*, 81(3), pp. 464–491, 1990.

- [11] Zghal, M., Bouali, H.-E., Lakhdar, Z. B., and Hamam, H., "The first steps for learning optics: Ibn Sahl's, Al-Haytham's and Young's works on refraction as typical examples," in *Education and Training in Optics and Photonics*, p. ESB2, Optical Society of America, 2007.
- [12] Deutscher Normenausschuß, editor, Schallabsorptionsgrad-Tabelle, Beuth-Vertrieb GmbH, Berlin, 1968.
- [13] Agrawal, S. and Braasch, J., "Impression of Spatially Distributed Reverberation in Multichannel Audio Reproduction," in *Audio Engineering Society Convention 145*, p. 10076, Audio Engineering Society, 2018.
- [14] Kuttruff, H., *Room Acoustics*, Spon Press, London, New York, 2000.
- [15] Meyer, J., "Raumakustik und Orchesterklang in den Konzertsälen Joseph Haydns," *Acta Acustica united with Acustica*, 41(3), pp. 145–162, 1978.
- [16] Herald staff, "Music will float from cistern to the heavens," 2008, August 14, Herald Net, Everett Herald and Sound Publishing, Inc., https://www.heraldnet.com/life/music-will-float-from-cistern-to-the-heavens/, last retrieved May 1, 2020.
- [17] Vorländer, M., Auralization: Fundamentals of Acoustics, Modelling, Simulation, Algorithms and Acoustic Virtual Reality, Springer, Berlin, Heidelberg, New York, 2008.